

DEEP BIOSPHERE

Exploring deep microbial life in coal-bearing sediment down to ~2.5 km below the ocean floor

F. Inagaki,^{1,2*} K.-U. Hinrichs,^{3*} Y. Kubo,^{4,5} M. W. Bowles,³ V. B. Heuer,³ W.-L. Hong,^{6†} T. Hoshino,^{1,2} A. Ijiri,^{1,2} H. Imachi,^{2,7} M. Ito,^{1,2} M. Kaneko,^{2,8} M. A. Lever,^{9‡} Y.-S. Lin,^{3§} B. A. Methé,¹⁰ S. Morita,¹¹ Y. Morono,^{1,2} W. Tanikawa,^{1,2} M. Bihan,¹⁰ S. A. Bowden,¹² M. Elvert,³ C. Glombitza,⁹ D. Gross,¹³ G. J. Harrington,¹⁴ T. Hori,¹⁵ K. Li,¹⁰ D. Limmer,^{12||} C.-H. Liu,¹⁶ M. Murayama,¹⁷ N. Ohkouchi,^{2,8} S. Ono,¹⁸ Y.-S. Park,^{19¶} S. C. Phillips,²⁰ X. Prieto-Mollar,³ M. Purkey,^{21#} N. Riedinger,^{22**} Y. Sanada,^{4,5} J. Sauvage,²³ G. Snyder,^{24††} R. Susilawati,²⁵ Y. Takano,^{2,8} E. Tasumi,⁷ T. Terada,²⁶ H. Tomaru,²⁷ E. Trembath-Reichert,²⁸ D. T. Wang,¹⁸ Y. Yamada,^{5,29}

Microbial life inhabits deeply buried marine sediments, but the extent of this vast ecosystem remains poorly constrained. Here we provide evidence for the existence of microbial communities in ~40° to 60°C sediment associated with lignite coal beds at ~1.5 to 2.5 km below the seafloor in the Pacific Ocean off Japan. Microbial methanogenesis was indicated by the isotopic compositions of methane and carbon dioxide, biomarkers, cultivation data, and gas compositions. Concentrations of indigenous microbial cells below 1.5 km ranged from <10 to $\sim 10^4$ cells cm^{-3} . Peak concentrations occurred in lignite layers, where communities differed markedly from shallower subseafloor communities and instead resembled organotrophic communities in forest soils. This suggests that terrigenous sediments retain indigenous community members tens of millions of years after burial in the seabed.

Microbial life has been found in marine sediments as deep as 1922 m below the seafloor (mbsf) (1), with cell numbers decreasing logarithmically as burial depth increases (2). However, the extent of the deep subseafloor biosphere and the factors limiting or stimulating life at its lower boundaries remain largely unknown, partly because of the technological challenges associated with obtaining pristine scientific samples from great depths. The deepest microbial signatures measured thus far come from the biodegradation of heavy oils in fossil fuel reservoirs down to subsurface depths of ~4 km (3, 4).

We studied the microbial communities associated with deep subseafloor coal beds, which are widespread along the Western Pacific continental margins (5). During Integrated Ocean Drilling Program (IODP) Expedition 337 in 2012, we drilled and recovered sediments down to 2466 mbsf using the riser-drilling vessel *Chikyu* at Site C0020, located along the northwestern Pacific margin (41°10.5983'N, 142°12.0328'E, 1180 m water depth) (fig. S1) (6). The top 365 mbsf of the borehole had been drilled in 2006 during the *Chikyu* cruise CK06-06 (6, 7). The site is located in the forearc basin offshore from the Shimokita Peninsula, Japan, where terrigenous sediments rich in organic matter were deposited in coastal environments during the late Paleogene to early Neogene periods, before the depositional environment became marine in the course of subsidence (5). The series of buried lignite coal beds at depths of ~1.5 to 2.5 km are 0.3 to 7.3 m thick (6). Because of the relatively low geothermal temperature gra-

dient of 24°C km^{-1} (6), the deepest horizons, with in situ temperatures of <60°C, are well within the thermal limits of microbial life.

We detected intact microbial cells throughout the entire drilled sediment column, down to the deepest sample at 2458 mbsf. Cell concentrations decreased with depth but in an unexpected fashion. In the “shallow” subseafloor (above 365 mbsf), concentrations decreased steadily from $\sim 10^9$ to $\sim 10^7$ cells cm^{-3} (8) and exceeded predictions based on the global regression line from previous surveys of cell concentrations at ocean margins (2) (Fig. 1A and table S1). In contrast, raw cellular concentrations were substantially lower in the “deep” subseafloor (below ~1.5 km), ranging from $\sim 10^2$ to 10^3 cells cm^{-3} , but they exceeded this range in coal-bearing horizons and adjacent sediment layers (Fig. 1A).

The low cell concentrations required the implementation of rigorous contamination tests to characterize indigenous microbial communities in the deep coal-bed biosphere. To minimize and quantify contamination potentially introduced during drilling, we (i) investigated whole round core sections by x-ray computed tomography before selecting sediment samples, (ii) took microbiological samples only from the center part of undisturbed core intervals, and (iii) quantified the intrusion of drill fluids into the cores by perfluorocarbon tracer assays (6, 7). As additional validation, we sequenced the V1 to V3 region of 16S ribosomal RNA genes in all sediment samples (7) obtained by riser drilling. We compared these to control samples consisting of drill mud and lab experimental blanks to differentiate in-

digenous microbial communities from contaminant cells (fig. S2) (7). We applied a probabilistic approach, incorporating taxon variability across samples to identify the likelihood that each taxon would be consistently sampled, either exclusively from the control or sediment sample sets or from both sample sets (7). In this way, we identified likely indigenous taxa, which were either (i) exclusive to sediment samples (“most conservative”) (figs. S2 to S4 and table S1) or (ii) consistently found in sediment samples in significant abundance and only occasionally found in

¹Kochi Institute for Core Sample Research, Japan Agency for Marine-Earth Science and Technology (JAMSTEC), Nankoku, Kochi 783-8502, Japan. ²Research and Development Center for Marine Resources, JAMSTEC, Yokosuka 237-0061, Japan. ³MARUM Center for Marine Environmental Sciences, University of Bremen, D-28359 Bremen, Germany. ⁴Center for Deep-Earth Exploration, JAMSTEC, Yokohama 236-0061, Japan. ⁵Research and Development Center for Ocean Drilling Science, JAMSTEC, Yokohama 236-0001, Japan. ⁶College of Earth, Ocean, and Atmospheric Sciences, Oregon State University, Corvallis, OR 97331, USA. ⁷Department of Subsurface Geobiological Analysis and Research, JAMSTEC, Yokosuka 237-0061, Japan. ⁸Department of Biogeochemistry, JAMSTEC, Yokosuka 237-0061, Japan. ⁹Center for Geomicrobiology, Department of Bioscience, Aarhus University, DK-8000 Aarhus C, Denmark. ¹⁰Department of Environmental Genomics, J. Craig Venter Institute, Rockville, MD 20850, USA. ¹¹Geological Survey of Japan, National Institute of Advanced Industrial Science and Technology (AIST), Tsukuba, Ibaraki 305-8567, Japan. ¹²Department of Geology and Petroleum Geology, School of Geosciences, University of Aberdeen, Aberdeen AB24 3UE, UK. ¹³Department of Applied Geosciences and Geophysics, Montanuniversität, 8700 Leoben, Austria. ¹⁴School of Geography, Earth and Environmental Sciences, University of Birmingham, Birmingham B15 2TT, UK. ¹⁵Environmental Management Research Institute, AIST, Tsukuba, Ibaraki 305-8569, Japan. ¹⁶The State Key Laboratory of Pharmaceutical Biotechnology, School of Life Science, Nanjing University, Nanjing, Jiangsu 210093, China. ¹⁷Center for Advanced Marine Core Research, Kochi University, Nankoku, Kochi 783-8502, Japan. ¹⁸Department of Earth, Atmospheric and Planetary Sciences, Massachusetts Institute of Technology, Cambridge, MA 02139, USA. ¹⁹Petroleum and Marine Resources Research Division, Korea Institute of Geoscience and Mineral Resources, Yuseong-gu, Daejeon 305-350, Korea. ²⁰Department of Earth Sciences, University of New Hampshire, Durham, NH 03824, USA. ²¹Department of Earth and Atmospheric Sciences, University of Nebraska-Lincoln, Lincoln, NE 68588, USA. ²²Department of Earth Sciences, University of California Riverside, Riverside, CA 92521, USA. ²³Graduate School of Oceanography, University of Rhode Island, Narragansett, RI 02882, USA. ²⁴Department of Earth Science, Rice University, Houston, TX 77005, USA. ²⁵School of Earth Science, University of Queensland, Brisbane Queensland 4072, Australia. ²⁶Marine Works Japan, Yokosuka 237-0063, Japan. ²⁷Department of Earth Sciences, Graduate School of Science, Chiba University, Chiba 263-8522, Japan. ²⁸Geological and Planetary Sciences, California Institute of Technology, Pasadena, CA 91125, USA. ²⁹Department of Urban Management, Graduate School of Engineering, Kyoto University, Kyoto 615-8540, Japan.

*Corresponding author. E-mail: inagaki@jamstec.go.jp (F.I.); khinrichs@uni-bremen.de (K.-U.H.) †Present address: CAGE - Centre for Arctic Gas Hydrate, Environment and Climate, Department of Geology, UiT The Arctic University of Norway, N-9037 Tromsø, Norway. ‡Present address: Department of Environmental Systems Science, ETH Zurich, 8092 Zurich, Switzerland. §Present address: Department of Oceanography, National Sun Yat-Sen University, Kaohsiung 80424, Taiwan. ||Present address: Adrok, Edinburgh, Scotland EH6 5NX, UK. ¶Deceased. #Present address: Noble Energy, 1625 Broadway, Suite 2200, Denver, CO 80202, USA. **Present address: Boone Pickens School of Geology, 105 Noble Research Center, Oklahoma State University, Stillwater, OK 74078-3031, USA. ††Present address: Gas Hydrate Research Laboratory, Meiji University, Tokyo 101-8301, Japan.

Downloaded from <http://science.sciencemag.org/> on October 8, 2018

contamination controls in low abundance (“most likely”) (figs. S5 and S6 and table S1). From this approach, we derived correction factors (table S1) to the raw cell concentrations to estimate the corresponding population sizes. We used the results of taxonomy-based sequence filtration and the probability-based relationship analysis for 16S sequences to estimate the “most conservative” and “most likely” indigenous cell concentrations, respectively (Fig. 1A, figs. S5 to S7, and table S1) (7). These estimated cell concentrations are much lower than predicted by the slope of the global regression line (fig. S7) (2) and are even lower than previously reported values from the most oligotrophic seafloor setting on Earth, the South Pacific Gyre (9).

Despite the very low cell numbers, geochemical data indicated microbial activity even in the deepest horizons sampled. Carbon isotopic compositions of methane ($\delta^{13}\text{C}\text{-CH}_4$) and ratios of methane over ethane (C_1/C_2) (Fig. 1, B and C), both continuously monitored in circulating mud gas during riser drilling (6), point to microbial methanogenesis as the predominant source of

methane (10) throughout the entire drilled sequence. Positive inflections of C_1/C_2 ratios between 1700 and 2000 mbsf suggest that biological methanogenesis is stimulated in coal-bearing horizons (Fig. 1C), where contamination-corrected cell concentrations reached $\sim 10^2$ to 10^4 cells cm^{-3} (Fig. 1A), as well as in the overlying 200 m of sediment. Hydrogen isotopic compositions of methane ($\delta\text{D}\text{-CH}_4$) ranged from -200 to -150 per mil (‰) (Fig. 1B), consistent with its production by hydrogenotrophic carbon dioxide (CO_2) reduction (10). Locally increased $\delta^{13}\text{C}\text{-CO}_2$ values in coal-bearing horizons provide further evidence that the CO_2 pool was isotopically fractionated by microbial methanogenesis (Fig. 1C). Moreover, in situ production of methane is indicated by the abundance of $^{13}\text{CH}_3\text{D}$ (a rare “clumped” isotopologue of methane with two heavy isotopes) in formation fluids sampled in two discrete coal-bed horizons (Fig. 1B and table S2) (6, 7). These analyses returned low $\Delta^{13}\text{CH}_3\text{D}\text{-T}$ -based temperatures of 70_{-9}^{+9}°C and 70_{-21}^{+24}°C (table S2), providing evidence against major contributions of more deeply sourced thermogenic methane, which

would be expected to carry clumped-isotope temperatures $>150\text{°C}$ (11). In addition, we detected coenzyme F_{430} in core samples, providing biomarker evidence for methanogenesis in coal beds ~ 2 km below the seafloor (Fig. 2A and table S3) (12, 13). Coenzyme F_{430} is a key prosthetic group of methyl-coenzyme M reductase that catalyzes the last step of methanogenesis. Its concentrations in deep sediments were about two orders of magnitude lower than in shallow sediments (table S3), suggesting the presence of a small but persistent community of methanogens in deep coal-bearing layers.

In a continuous-flow bioreactor (14) at near in situ temperature (40°C), we enriched methanogenic communities from ~ 2 -km-deep coal-bed samples amended with powdered coal as the major energy source (7) (Fig. 2, B to G). Analysis of methyl-coenzyme M reductase gene (*mcrA*) sequences in this enrichment culture indicated the growth of hydrogenotrophic methanogens closely related to *Methanobacterium subterraneum* and *M. formicicum* (fig. S8). These species have previously been detected in terrestrial coal beds (15)

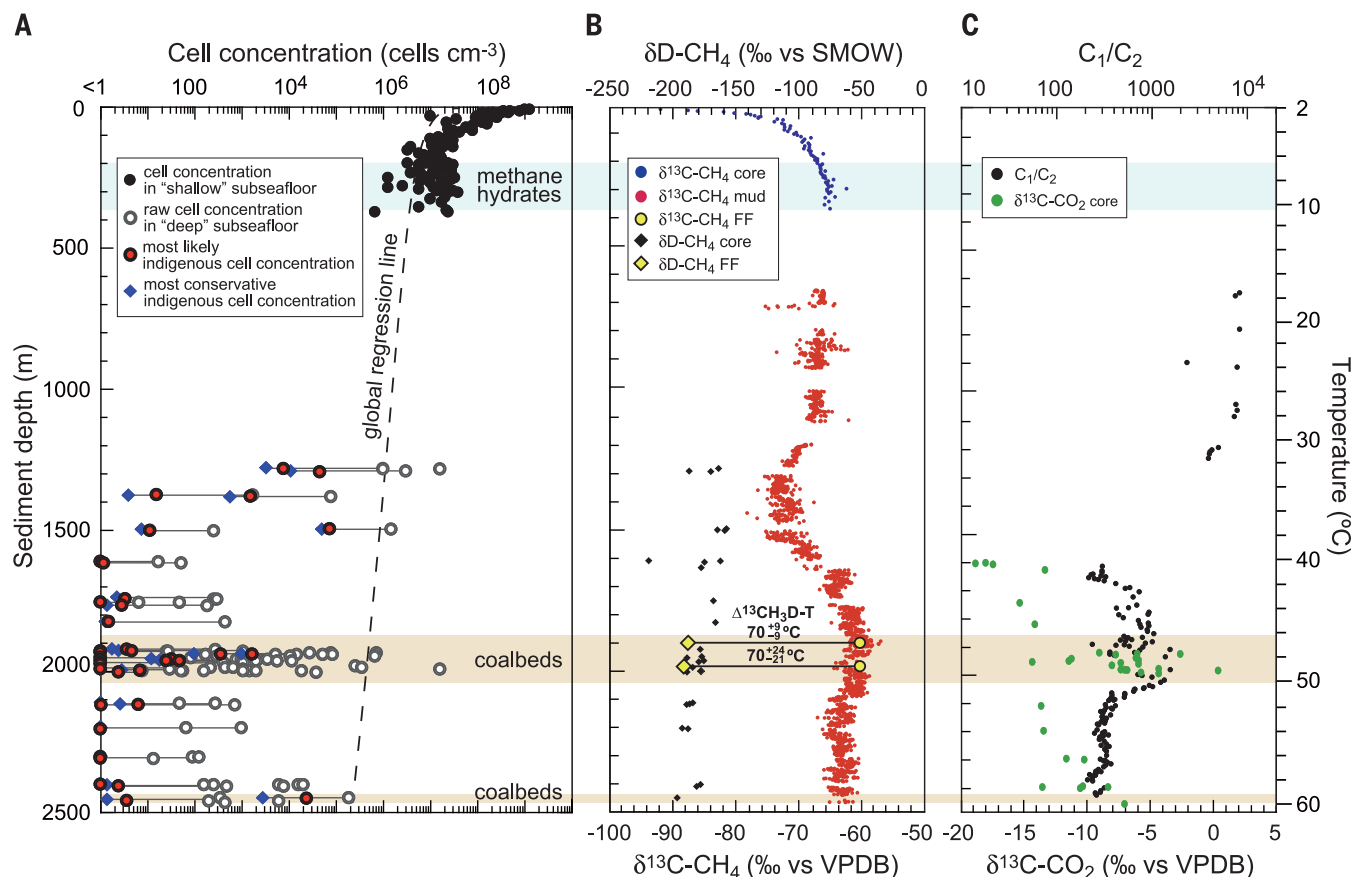


Fig. 1. Depth profiles of microbial cell counts and geochemical data at Site C0020. (A) Microbial cell concentrations, (B) $\delta^{13}\text{C}$ and δD of methane, and (C) C_1/C_2 ratios and $\delta^{13}\text{C}$ of CO_2 . (A) For cell concentrations in the deep subseafloor, raw data of fluorescence image-based cell counts (8), the most likely indigenous cell concentrations based on the probability-relationship set analysis (7), and the most conservative indigenous cell concentrations estimated based on the taxonomic classification (7) are shown (figs. S6 and S7 and table S1). The correction factor is the proportion of sequences estimated to be indigenous (table S1). The

minimal quantification limit for raw cell counts was 1.43×10^2 cells cm^{-3} (i.e., the upper 95% confidence interval of the negative background). All $\delta^{13}\text{C}$ and δD in (B) and (C) are in per mil versus the Vienna Pee Dee Belemnite (VPDB) and Standard Mean Ocean Water (SMOW) standards, respectively. The $\Delta^{13}\text{CH}_3\text{D}\text{-T}$ values in (B) designate the apparent equilibrium temperatures derived from measurements of $^{13}\text{CH}_3\text{D}$, a clumped isotopologue of methane (table S2) in discrete formation fluid (FF) samples (6, 7). Temperature is based on the temperature gradient of 24°C km^{-1} determined by downhole logging (6).

and in shallower, methane hydrate-bearing sediments at Site C0020 (14). Using nanoscale secondary ion mass spectrometry (NanoSIMS) (7, 16), we detected the incorporation of ^{13}C -labeled bicarbonate into cellular biomass (Fig. 2, E to G). Collectively, these microbiological and geochemical findings indicate that microbial communities are stimulated within coal-bed environments and that hydrogenotrophic methanogens act as terminal remineralizers.

Despite these multiple lines of evidence for the activity of methanogenic archaea, we could only

amplify one archaeal 16S sequence related to *Methanosarcina barkeri* (from a ~2-km-deep coal sample) and one *mcrA* sequence related to *Methanococcus maripaludis* (from ~1-km-deep cuttings samples) (fig. S8) (7). Archaeal 16S genes were neither quantifiable by digital polymerase chain reaction (dPCR) (17) nor stably amplifiable using multiple primer sets, indicating that this deep subsurface microbial ecosystem harbors substantially lower proportions of archaea than shallower sediments at this and other ocean margin sites (18). The difficulty in detecting meth-

anogenic archaea using multiple molecular assays is not unexpected, given their generally low relative abundance of <1%, even in methane-laden subsurface sediments (19).

The taxonomic distribution based on 16S sequences of the most conservative indigenous community members showed a marked difference between bacterial communities in deeper layers (1279.1 to 2458.8 mbsf) and those in shallower layers (9.5 to 364.0 mbsf) (Fig. 3, figs. S3 and S4, and table S4). For example, in deeper layers, sequences affiliated with the phyla Chloroflexi or

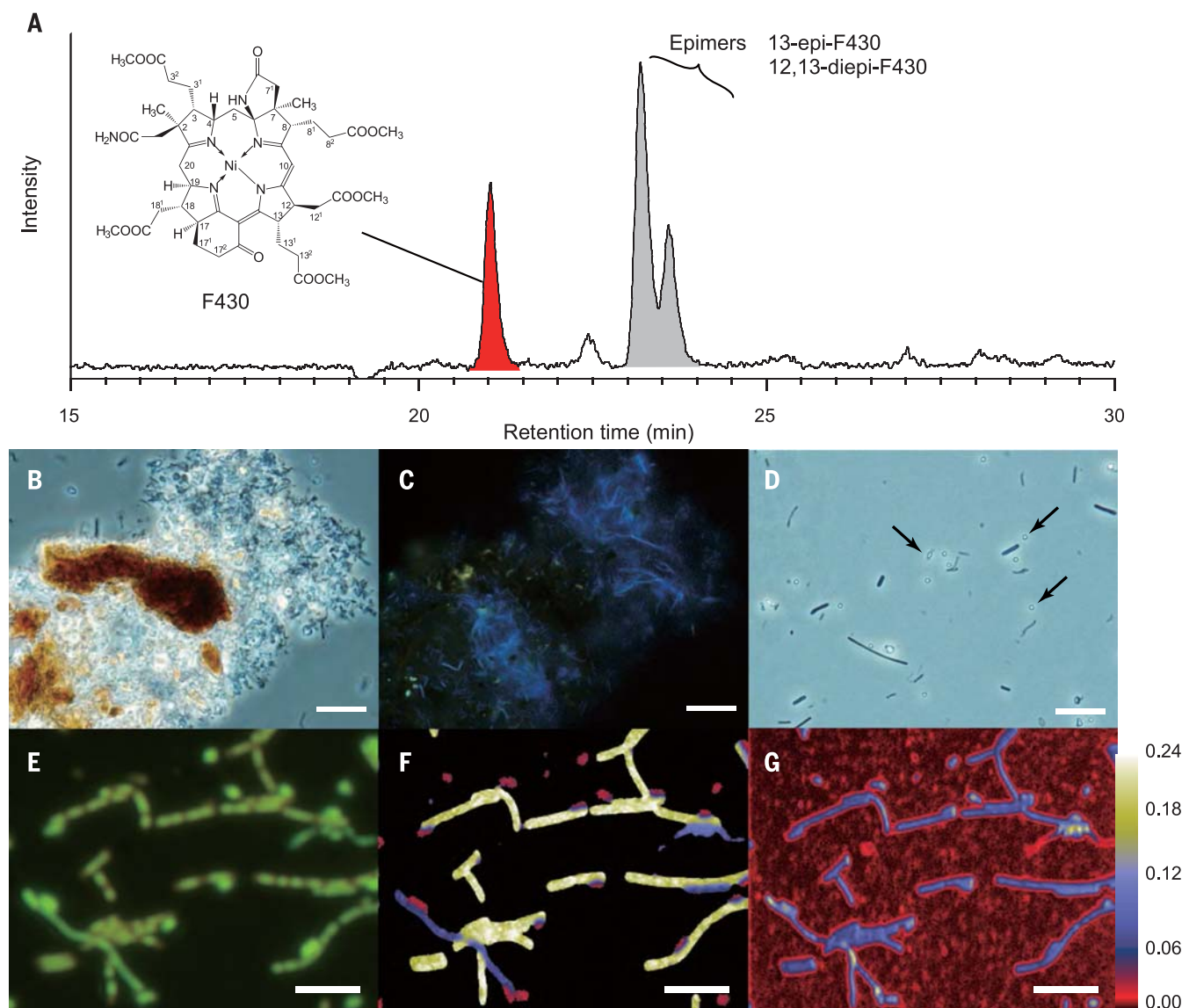


Fig. 2. Geochemical and microbiological indications for methanogenic microbial communities in ~2-km-deep subsurface coal beds at Site C0020.

(A) A representative chromatogram of the diagnostic methanogen biomarker F_{430} (as methyl ester) and its epimers from a coal sample (core 18R-2, 1946 mbsf) (table S3). (B) to (D) Photomicrographs of microbial cells in an enrichment culture from ~2-km-deep coal-bed samples using a continuous-flow bioreactor with powdered coal as the major energy source (7). (B) Phase-contrast micrograph of microbial cells attached to mineral particles. (C)

Fluorescent micrograph of the same field shown in (B) showing the growth of methanogens that produce autofluorescence derived from coenzyme F_{420} . (D) Phase-contrast micrograph showing spherical spore-like particles, indicated by arrows. (E) to (G) NanoSIMS analysis of cells in the reactor enrichment culture incubated with ^{13}C -labeled bicarbonate (7). (E) Fluorescent micrograph of SYBR Green I-stained cells. (F) and (G) NanoSIMS ion images of $^{13}\text{C}/^{12}\text{C}$ (F) and ^{12}C (G). The color gradient indicates the relative abundance of ^{13}C expressed as $^{13}\text{C}/^{12}\text{C}$. The length of the bars is 10 μm .

“Atribacteria” [candidate division JS1 (20, 21)], which are both globally abundant groups in sub-seafloor sediments at ocean margins (22, 23), were detected in lower proportions than in shallower layers (Fig. 3A, fig. S3, and table S4). The indigenous sequence assemblage in deeper layers was dominated instead by bacterial groups known to dominate a wide range of terrestrial soil environments (Actinobacteria, Proteobacteria, Firmicutes, Bacteroidetes, and Acidobacteria) (24). In fact, many operational taxonomic units (OTUs) from deeper layers showed high sequence similarity to those from forest soils (figs. S3 and S4). Deeper layers also included microbial phyla that were not or were only barely detectable in shallower layers (such as Gemmatimonadetes and Synergistetes) (fig. S9) (7). Clustering and Bray-Curtis dissimilarity analyses (Fig. 3B and fig. S10), as well as multidimensional scaling and permutational analysis of variance based on genus-level classification (fig. S11), further support the notion that deep communities in coal-associated sedimentary environments on the former forearc basin off Shimokita differ compositionally from those found in shallow diatom-rich marine sediments.

Our combined microbiological and geochemical data set provides an opportunity to examine the potential energy sources of life at depths greater than ~1.5 km below the seafloor. The concentration of dissolved hydrogen (H_2), a key intermediate in the anaerobic degradation of organic matter, is an important gauge of the bioenergetic status of anaerobic microbial ecosystems (25, 26). At Site C0020, high H_2 concentrations of ~1 to ~500 μM in sediments below 1.5 km (fig. S12 and table S5) resulted in Gibbs free energy yields of hydrogenotrophic methanogenesis that were much more negative than those previously documented from energy-rich surface environments (fig. S13 and tables S6 and S7) (25). These high H_2 concentrations suggest very low H_2 turnover rates, possibly due to low concentrations of microorganisms with low viabilities and consequently low cell-specific energy turnover. Under these circumstances, the coupling between substrate production and substrate uptake may be severely delayed, resulting in long residence times and the accumulation of H_2 to high concentrations in sediment porewater. These substrates are probably generated from lignite (15), micro-

bial necromass (27), and/or adsorbed organic matter. In addition to enzymatic hydrolysis, chemical degradation of recalcitrant organic matter (28, 29) in situ and in deeper, warmer strata bearing Cretaceous coal beds (30) may supply monomeric substrates and contribute to the accumulation of H_2 . Despite the high H_2 concentrations, a range of organotrophic reactions involving the breakdown of lignin phenols, cellular building blocks, and anaerobic degradation intermediates are likely to be thermodynamically favorable and thus could explain the presence of alive and active microbial populations (fig. S13).

In addition to energy availability from organotrophic and hydrogenotrophic reactions, an important factor controlling the viability and size of microbial communities buried deeper than 1.5 km could be the increase in energy expended on the repair of biomolecules as a function of depth. The rates of abiotic amino acid racemization and DNA depurination increase exponentially with temperature (31), and substantial increases in their modeled rates coincided with a dramatic drop in cell numbers at Site C0020 (fig. S14). The relatively increased energetic cost of biomolecule repair

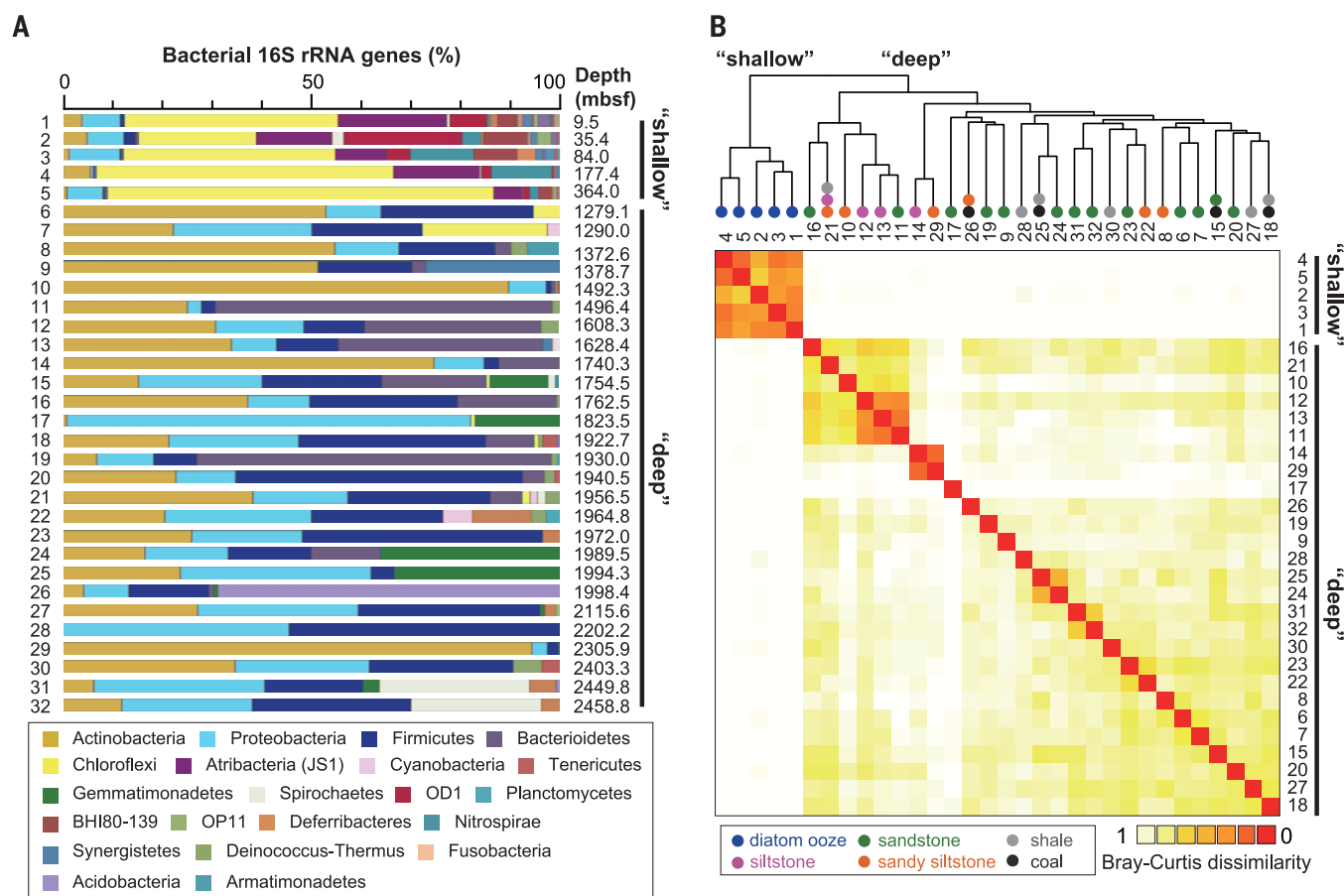


Fig. 3. Taxonomic distribution of the most conservative indigenous bacterial communities in sediments at Site C0020. (A) Phylum-level taxonomic composition of bacterial 16S gene-tagged sequences (i.e., V1–V3 region) in shallow (sample numbers 1 to 5, 9.5 to 364 mbsf, from *Chikyu* cruise CK06-06) and deep (sample numbers 6 to 32, 1279.1 to 2458.8 mbsf, from IODP Expedition 337) subseafloor sediment samples (7). (B) Cluster

and Bray-Curtis dissimilarity analyses of bacterial community structure based on the genus-level classification of the same sequence assemblages used in (A). Colored dots on the cluster tree represent the sedimentological characteristics of each sample horizon (6). The OTU-based analysis for the most likely indigenous bacterial communities in deep subseafloor sediment samples is shown in fig. S10.

could result in a higher cell-specific energy demand in the deeper layers at Site C0020 and may explain why microbial abundance was only a small fraction of the size predicted by the global regression line (Fig. 1A and figs. S7 and S14).

Our findings provide a comprehensive view of the deep seafloor biosphere associated with coal beds. Despite energetic challenges, this environment appears to have maintained some of the taxonomic groups that populated the original shallow depositional setting and have contributed to carbon cycling ever since.

REFERENCES AND NOTES

1. M.-C. Ciobanu et al., *ISME J.* **8**, 1370–1380 (2014).
2. R. J. Parkes, B. A. Cragg, P. Wellsbury, *Hydrogeol. J.* **8**, 11–28 (2000).
3. I. M. Head, D. M. Jones, S. R. Larter, *Nature* **426**, 344–352 (2003).
4. D. M. Jones et al., *Nature* **451**, 176–180 (2007).
5. A. I. Konyukhov, *Lithol. Miner. Resour.* **45**, 465–485 (2010).
6. Expedition 337 Scientists, in *Proceedings of the Integrated Ocean Drilling Program*, F. Inagaki, K.-U. Hinrichs, Y. Kubo, Eds. (IODP Management International, Tokyo, vol. 337, 2013); <http://publications.iodp.org/proceedings/337/103/103.htm>.
7. Materials and methods are available as supplementary materials on Science Online.
8. Y. Morono, T. Terada, N. Masui, F. Inagaki, *ISME J.* **3**, 503–511 (2009).
9. S. D'Hondt et al., *Nat. Geosci.* **8**, 299–304 (2015).
10. M. J. Whiticar, *Chem. Geol.* **161**, 291–314 (1999).
11. D. A. Stolper et al., *Science* **344**, 1500–1503 (2014).
12. M. Kaneko et al., *Anal. Chem.* **86**, 3633–3638 (2014).
13. Y. Takano et al., *Org. Geochem.* **58**, 137–140 (2013).
14. H. Imachi et al., *ISME J.* **5**, 1913–1925 (2011).
15. D. Strapoć et al., *Annu. Rev. Earth Planet. Sci.* **39**, 617–656 (2011).
16. Y. Morono et al., *Proc. Natl. Acad. Sci. U.S.A.* **108**, 18295–18300 (2011).
17. T. Hoshino, F. Inagaki, *Syst. Appl. Microbiol.* **35**, 390–395 (2012).
18. J. S. Lipp, Y. Morono, F. Inagaki, K.-U. Hinrichs, *Nature* **454**, 991–994 (2008).
19. F. S. Colwell et al., *Appl. Environ. Microbiol.* **74**, 3444–3452 (2008).
20. G. Webster, R. J. Parkes, J. C. Fry, A. J. Weightman, *Appl. Environ. Microbiol.* **70**, 5708–5713 (2004).
21. J. A. Dodsworth et al., *Nat. Commun.* **4**, 1854 (2013).
22. F. Inagaki et al., *Proc. Natl. Acad. Sci. U.S.A.* **103**, 2815–2820 (2006).
23. A. P. Teske, *Geomicrobiol. J.* **23**, 357–368 (2006).
24. N. Fierer, M. A. Bradford, R. B. Jackson, *Ecology* **88**, 1354–1364 (2007).
25. T. M. Hoehler, M. J. Alperin, D. B. Albert, C. S. Martens, *Geochim. Cosmochim. Acta* **62**, 1745–1756 (1998).
26. B. Schink, *Microbiol. Mol. Biol. Rev.* **61**, 262–280 (1997).
27. B. A. Lomstein, A. T. Langerhuus, S. D'Hondt, B. B. Jørgensen, A. J. Spivack, *Nature* **484**, 101–104 (2012).
28. B. Horsfield et al., *Earth Planet. Sci. Lett.* **246**, 55–69 (2006).
29. R. J. Parkes et al., *Org. Geochem.* **38**, 845–852 (2007).
30. M. Osawa, S. Nakanishi, M. Tanahashi, H. Oda, *J. Japan. Assoc. Pet. Technol.* **67**, 38–51 (2002).
31. M. A. Lever et al., *FEMS Microbiol. Rev.* 10.1093/femsre/fuv020 (2015).

ACKNOWLEDGMENTS

The authors are grateful to IODP and the Ministry of Education, Culture, Sports, Science and Technology of Japan for providing an opportunity to explore the deep coal-bed biosphere off Shimokita during Expedition 337. We thank all crews, drilling team members, lab technicians, and scientists on the drilling vessel *Chikyu* for supporting core sampling and onboard measurements during *Chikyu* shakedown cruise CK06-06 and IODP Expedition 337. The authors thank J. A. McKenzie and K. H. Nealson for useful discussions during project design; S. Fukunaga, S. Hashimoto, A. Imajo, Y. Saito, S. Tanaka, K. Uematsu, and N. Xiao for assistance in microbiological analyses; and D. Gruen for technical assistance during clumped isotope analysis. This work was supported in part by the Japan Society for the Promotion of Science (JSPS) Strategic Fund for

Strengthening Leading-Edge Research and Development (to F.I. and JAMSTEC), the JSPS Funding Program for Next Generation World-Leading Researchers (grant no. GR102 to F.I.), the JSPS Grants-in-Aid for Science Research (no. 26251041 to F.I., no. 24770033 to T.H., no. 24687011 to H.I., no. 26287142 to M.I., no. 25610166 to M.K., and nos. 24651018 and 24687004 to Y.M.), the European Research Council (Advanced Grant no. 247153 to K.-U.H.), the Deutsche Forschungsgemeinschaft through project HI 616/16 (to K.-U.H.) through MARUM-Cluster of Excellence 309, and NSF (no. EAR-1250394 to S.O.). All shipboard and shore-based data presented in this manuscript are archived and publicly available online in the IODP Expedition 337 Proceedings (6) through the J-CORES database (<http://sio7.jamstec.go.jp/j-cores.data/337/>

C0020A/) and the PANGAEA database (<http://doi.pangaea.de/10.1594/PANGAEA.845984>). This is a contribution to the Deep Carbon Observatory.

SUPPLEMENTARY MATERIALS

www.sciencemag.org/content/349/6246/420/suppl/DC1
Materials and Methods
Figs. S1 to S14
Tables S1 to S7
References (32–83)

23 January 2015; accepted 10 June 2015
10.1126/science.aaa6882

NEURODEVELOPMENT

Adult cortical plasticity depends on an early postnatal critical period

Stuart D. Greenhill,^{1,*} Konrad Juczewski,^{2,*} Annelies M. de Haan,¹ Gillian Seaton,¹ Kevin Fox,¹ Neil R. Hardingham^{1†}

Development of the cerebral cortex is influenced by sensory experience during distinct phases of postnatal development known as critical periods. Disruption of experience during a critical period produces neurons that lack specificity for particular stimulus features, such as location in the somatosensory system. Synaptic plasticity is the agent by which sensory experience affects cortical development. Here, we describe, in mice, a developmental critical period that affects plasticity itself. Transient neonatal disruption of signaling via the C-terminal domain of “disrupted in schizophrenia 1” (DISC1)—a molecule implicated in psychiatric disorders—resulted in a lack of long-term potentiation (LTP) (persistent strengthening of synapses) and experience-dependent potentiation in adulthood. Long-term depression (LTD) (selective weakening of specific sets of synapses) and reversal of LTD were present, although impaired, in adolescence and absent in adulthood. These changes may form the basis for the cognitive deficits associated with mutations in DISC1 and the delayed onset of a range of psychiatric symptoms in late adolescence.

Disrupted in schizophrenia 1 (DISC1) is a protein that, when mutated, predisposes the human carrier for a number of mental disorders including schizophrenia, bipolar disorder, recurrent major depression, and autism (*1, 2*). DISC1 interacts with a surprisingly large number of signaling molecules, including phosphodiesterase 4, glycogen synthase kinase 3, kalirin-7, fasciculation and elongation protein ζ 1, kndrin, lissencephaly 1 (Lis1), and nudeE neurodevelopment protein 1-like 1 (Nudel) (*3–8*). DISC1 affects diverse aspects of neuronal development, such as proliferation, migration, and neurite extension. In addition, DISC1 is known to be expressed in cortical neurons during both development and adulthood (*9*) and to reside at the postsynaptic density (*6, 10–12*), although very little is understood of the role it plays there. In this study, working with mice, we asked whether DISC1 protein-protein interactions early in development are critical for synaptic

plasticity in adulthood. We disrupted transiently DISC1's interaction with Lis1 and Nudel during early development, at a time after cortical neurogenesis and cell migration [which are complete by about postnatal day 7 (P7) in the mouse] but before synaptogenesis and dendrite formation dominate.

We studied adult plasticity in the mouse barrel cortex, a primary sensory cortical area that receives tactile information from a normal array of 40 large whiskers. We removed all but one whisker on one side of the face of adult mice (*13*) to invoke cortical plasticity. The single-whisker experience normally leads to expansion of the cortical territory responding to the spared whisker (Fig. 1A). To manipulate DISC1 interactions with Lis1 and Nudel, we used a conditional transgenic mouse expressing the DISC1 C-terminal domain (DISC1cc; residues 671 to 852), which interacts with Lis1 and Nudel (*14–16*) in a tamoxifen-sensitive construct. Within this system, a single tamoxifen injection affects DISC1 signaling for 6 to 48 hours (P7 to P9) (*15*). Spatial expression of DISC1cc is restricted to excitatory neurons in the forebrain by the calcium/calmodulin-dependent protein kinase II subunit α (α CaMKII) promoter, and its activity is controlled by tamoxifen. We studied

¹School of Biosciences, Cardiff University, Cardiff, CF23 3AX, UK. ²National Institute on Alcohol Abuse and Alcoholism, NIH, Rockville, MD 20852, USA.

*These authors contributed equally to this work. †Corresponding author. E-mail: sbinrh@cardiff.ac.uk

Exploring deep microbial life in coal-bearing sediment down to ~2.5 km below the ocean floor

F. Inagaki, K.-U. Hinrichs, Y. Kubo, M. W. Bowles, V. B. Heuer, W.-L. Hong, T. Hoshino, A. Ijiri, H. Imachi, M. Ito, M. Kaneko, M. A. Lever, Y.-S. Lin, B. A. Methé, S. Morita, Y. Morono, W. Tanikawa, M. Bihan, S. A. Bowden, M. Elvert, C. Glombitza, D. Gross, G. J. Harrington, T. Hori, K. Li, D. Limmer, C.-H. Liu, M. Murayama, N. Ohkouchi, S. Ono, Y.-S. Park, S. C. Phillips, X. Prieto-Mollar, M. Purkey, N. Riedinger, Y. Sanada, J. Sauvage, G. Snyder, R. Susilawati, Y. Takano, E. Tasumi, T. Terada, H. Tomaru, E. Trembath-Reichert, D. T. Wang and Y. Yamada

Science **349** (6246), 420-424.
DOI: 10.1126/science.aaa6882

A deep sleep in coal beds

Deep below the ocean floor, microorganisms from forest soils continue to thrive. Inagaki *et al.* analyzed the microbial communities in several drill cores off the coast of Japan, some sampling more than 2 km below the seafloor (see the Perspective by Huber). Although cell counts decreased with depth, deep coal beds harbored active communities of methanogenic bacteria. These communities were more similar to those found in forest soils than in other deep marine sediments.

Science, this issue p. 420; see also p. 376

ARTICLE TOOLS

<http://science.sciencemag.org/content/349/6246/420>

SUPPLEMENTARY MATERIALS

<http://science.sciencemag.org/content/suppl/2015/07/22/349.6246.420.DC1>

RELATED CONTENT

<http://science.sciencemag.org/content/sci/349/6246/376.full>

REFERENCES

This article cites 75 articles, 13 of which you can access for free
<http://science.sciencemag.org/content/349/6246/420#BIBL>

PERMISSIONS

<http://www.sciencemag.org/help/reprints-and-permissions>

Use of this article is subject to the [Terms of Service](#)